Progress In Electromagnetics Research, PIER 33, 299–331, 2001

MODELING OF RECTANGULAR WAVEGUIDE JUNCTIONS CONTAINING CYLINDRICAL POSTS

M. El Sabbagh and K. Zaki

University of Maryland
Electrical & Computer Engineering Department
College Park, MD 20742, USA

Abstract—Accurate determination of the generalized scattering matrix of the crossed waveguides junction, T-junction and right-angle bend containing a cylindrical post is presented. The generalized scattering matrix of the four port structure is obtained from those of the two ports right angle bend with different combinations of perfect electric and/or magnetic walls. The generalized scattering matrix of the right angle bend (quarter of the structure) is obtained by the mode matching method where the electromagnetic fields in rectangular waveguides are matched to those in a junction section formed by a sectoral region.

1. INTRODUCTION

Conducting and dielectric cylindrical objects in rectangular waveguide junctions such as crossed waveguides junction, T-junction and right-angle bend play a very important role in RF/microwave filters, multiplexers and power dividers [1, 2]. To design such microwave structures, it is essential to model a cylindrical object in a rectangular waveguide junction as a key building block and to obtain the generalized scattering matrix. A cascading procedure using generalized scattering matrices [3–6] is applied to solve very complicated problems encountered in filter design and many other applications regardless of whether the cylindrical object is in a propagating or in a cut-off waveguide. Mode matching is a powerful method for obtaining generalized scattering matrices and has been successfully applied to model cylindrical dielectric posts in rectangular waveguides [7–11].

The symmetrical crossed waveguides junction, shown in Fig. 1, is first analyzed. Generalized scattering matrices of many structures such as T-junction, right angle bend, rectangular waveguide and one port structure can be derived from the crossed waveguides junction. It is assumed that all the ports have the same cross section dimensions. By short circuiting one port the generalized scattering matrix of a T-junction is obtained. Similarly by short circuiting two adjacent ports the Right-angle bend is obtained. By short circuiting two opposite ports, the rectangular waveguide is obtained and by short circuiting three ports, a one port structure is obtained. Taking into consideration the symmetrical properties of the crossed waveguide junction only one quarter of the structure need to be analyzed. The generalized scattering parameters of the crossed waveguides junction can be obtained from four sets of two ports generalized scattering parameters obtained by bisecting the junction at the symmetry planes using combination of perfect electric wall (PEW) and perfect magnetic wall (PMW). Four cases are analyzed: PEW-PEW, PEW-PMW, PMW-PEW, PMW-PMW, where the first wall is placed at the vertical plane of symmetry and the second wall is placed at the horizontal plane of symmetry. Since the cases of PMW-PEW or PEW-PMW are the same, it is sufficient to analyze 3 different cases of two ports structures from which the generalized scattering matrix of the crossed waveguides junction is obtained.

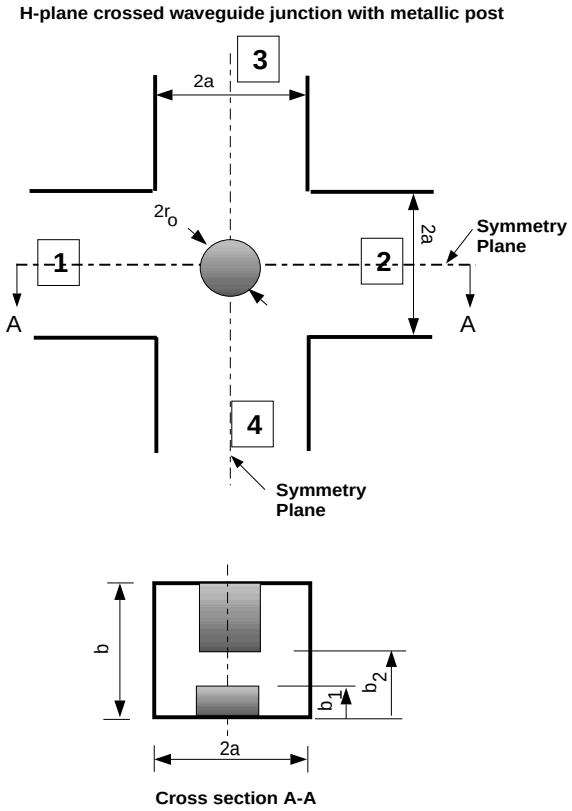

Figure 1. Crossed H-plane waveguides.

2. ANALYSIS

Consider a quarter of the structure which is a right-angle bend with a quarter post inside as shown in Fig. 2. The cylindrical post is assumed to be a perfect conductor. It has a radius r_0, and extends partially from the bottom and the top walls of the guide with a gap b_g equal to $(b_2 - b_1)$. The quarter of the structure, shown in Fig. 2, is divided into four regions. Two cylindrical regions:

$$\text{Region } I: \qquad \rho \le r_0, \quad 0 \le \phi \le \frac{\pi}{2}$$

$$\text{Region } II: \qquad r_0 \le \rho \le r_1, \quad r_1 = \sqrt{2}a, \quad 0 \le \phi \le \frac{\pi}{2}$$

and two waveguide regions W_1 and W_2.

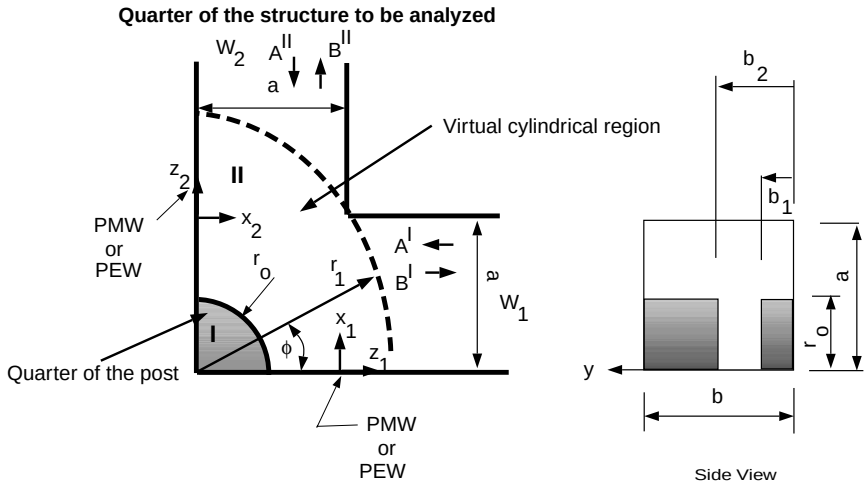

Figure 2. Quarter of the structure analyzed at a time with the different regions.

2.1. Field Expressions in Radial Waveguide Region

The electromagnetic fields in the cylindrical regions (*I, II*) are expanded in terms of TE_y and TM_y radial waveguide modes, satisfying the boundary conditions on the post, top, bottom of the waveguide and the surfaces $\phi = 0,\ \phi = 90^\circ$ [11]. Table 1 indicates the type of walls at $\phi = 0, 90^\circ$ and the radial waveguide modes needed in the field expansions. It is to be noted that the superscripts c and s in this table refer to the $\phi-$ variations of $\cos n\phi$ and $\sin n\phi$ respectively.

Table 1. Type of wall, corresponding modes used in the cylindrical region.

$\mathrm{TE}_y^c,\ \mathrm{TM}_y^s$	PEW-PEW
$\mathrm{TE}_y^s,\ \mathrm{TM}_y^c$	PMW-PMW
$\mathrm{TE}_y^c,\ \mathrm{TM}_y^s$	PMW-PEW
$\mathrm{TE}_y^s,\ \mathrm{TM}_y^c$	PEW-PMW

To apply the mode matching method in the radial direction [24, 25], the transverse fields with respect to ρ direction in each cylindrical region are expanded in terms of cylindrical eigenmodes. Explicit expressions for the expansions are given in Appendix A.

2.2. Field Expressions in the Rectangular Waveguide Regions

In the rectangular waveguide regions ($W_1,\ W_2$) in Fig. 2, the transverse fields with respect to the radial direction are linear combinations of the transverse fields TE and TM waveguide eigenmodes including both forward (F) and backward (B) waves. Explicit expressions for the field expansions and the eigenmodes are given in Appendix B.

2.3. Modeling of the Generalized Scattering Matrix

To complete the mode matching analysis, the boundary conditions have to be satisfied along two cylindrical boundaries $\rho = r_0$ and $\rho = r_1$ as shown in Fig. 2. Enforcing the continuity of the tangential fields at the boundary $\rho = r_0$ and properly defining the inner products, one can readily obtain a matrix equation with the following form

$$\left[\left[M_C^{II}\right]\ \left[M_D^{II}\right]\right]\left[\begin{array}{c}\mathbf{C}^{II}\\ \mathbf{D}^{II}\end{array}\right] = 0 \tag{1}$$

$\mathbf{C^{II}}$ and $\mathbf{D^{II}}$ are the field coefficients vectors with element C_{nm}^{IIv} and $D_{nm}^{IIv}(v = e, h)$, respectively. $\left[M_C^{II}\right]$ and $\left[M_D^{II}\right]$ are diagonal block matrices of size $N_C^{II} \times N_C^{II}$, where N_C^{II} is the total number of eigenmodes used in cylindrical region *II*. Each block matrix corresponds to the inner products of the eigenmodes with the same ϕ variations.

Since both region *I* and region *II* are cylindrical regions, mode orthogonality can be applied and all the inner products can be obtained analytically. At the artificial boundary $\rho = r_1$, the field continuity requires

$$\vec{E}_{ct}^{II}(r_1, \phi, y) = \delta_w^{(1)}(\phi)\vec{E}_{wt}^{(1)}(x_1, y, z_1) + \delta_w^{(2)}(\phi)\vec{E}_{wt}^{(2)}(x_2, y, z_2) \tag{2}$$

$$\vec{H}_{ct}^{II}(r_1, \phi, y) = \delta_w^{(1)}(\phi)\vec{H}_{wt}^{(1)}(x_1, y, z_1) + \delta_w^{(2)}(\phi)\vec{H}_{wt}^{(2)}(x_2, y, z_2) \tag{3}$$

where

$$\begin{aligned}\delta_w^{(1)} &= \left\{\begin{array}{ll} 1 & 0 < \phi \le \dfrac{\pi}{4} \\ 0 & \dfrac{\pi}{4} < \phi \le \dfrac{\pi}{2} \end{array}\right\} \\ \delta_w^{(2)} &= \left\{\begin{array}{ll} 0 & 0 < \phi \le \dfrac{\pi}{4} \\ 1 & \dfrac{\pi}{4} < \phi \le \dfrac{\pi}{2} \end{array}\right\}\end{aligned} \tag{4}$$

Taking cross inner product to (2) and (3) with $\vec{h}_{ctn'm'}$ and $\vec{e}_{ctn'm'}$, respectively and truncating the summations in the equations to appropriate finite numbers, the following equations are obtained

$$\begin{aligned}\left[\Lambda_{EJ}^{II}\right]\mathbf{C}^{II}+\left[\Lambda_{EY}^{II}\right]\mathbf{D}^{II} &= \left[T_E^{(1)B}\right]\mathbf{A}^{(1)}+\left[T_E^{(1)F}\right]\mathbf{B}^{(1)} \\ &\quad +\left[T_E^{(2)F}\right]\mathbf{A}^{(2)}+\left[T_E^{(2)B}\right]\mathbf{B}^{(2)} \quad (5)\\ \left[\Lambda_{HJ}^{II}\right]\mathbf{C}^{II}+\left[\Lambda_{EY}^{II}\right]\mathbf{D}^{II} &= \left[T_H^{(1)B}\right]\mathbf{A}^{(1)}+\left[T_H^{(1)F}\right]\mathbf{B}^{(1)} \\ &\quad +\left[T_H^{(2)F}\right]\mathbf{A}^{(2)}+\left[T_H^{(2)B}\right]\mathbf{B}^{(2)} \quad (6)\end{aligned}$$

Where $\mathbf{A}^{\imath}$ and $\mathbf{B}^{\imath}$ are vectors of size $N_W^{\imath}(\imath=1,2)$, $N_W^{(\imath)}$ is the total number of modes used in waveguide region $\imath$, containing the field coefficients of the incident and reflected eigenwaves in region $\imath$ of the rectangular waveguide. Matrices $\left[\Lambda_{EZ}^{II}\right]$, and $\left[\Lambda_{EZ}^{II}\right](Z=J,Y)$ are diagonal matrices of size $N_C^{II}\times N_C^{II}$ and their elements are determined by the self inner products in region II and are given by:

$$(\Lambda_{EZ}^{q})=\begin{cases}\dfrac{Z_n\left(\xi_m^{qp}r_1\right)}{Z_n\left(\xi_m^{qp}r_0\right)} & \text{if } p=e \text{ for } j\text{-th mode}\\ \dfrac{Z_n'\left(\xi_m^{qp}r_1\right)}{Z_n'\left(\xi_m^{qp}r_0\right)} & \text{if } p=h \text{ for } j\text{-th mode}\end{cases} \qquad Z\in J,Y \quad q=II \quad (7)$$

$$(\Lambda_{HZ}^{q})=\begin{cases}\dfrac{|\xi_m^{qp}|\,Z_n\left(\xi_m^{qp}r_2\right)}{Z_n\left(\xi_m^{qp}r_0\right)} & \text{if } p=e \text{ for } j\text{-th mode}\\ \dfrac{Z_n'\left(\xi_m^{qp}r_0\right)}{|\xi_m^{qp}|\,Z_n'\left(\xi_m^{qp}r_0\right)} & \text{if } p=h \text{ for } j\text{-th mode}\end{cases} \qquad Z\in J,Y\ q=II \quad (8)$$

$\left[T_E^{(\imath)V}\right]$ and $\left[T_H^{(\imath)V}\right]$ $(V=F,B)$ are sparse matrices of size $N_C^{II}\times N_W^{(\imath)}$ $(\imath=1,2)$. The mutual inner products of the eigenmodes (with the same y-variations in the waveguide regions and the cylindrical region II) determine the nonzero elements of the matrices which are stated as:

$$\begin{aligned}\left(T_E^{(\imath)V}\right)_{kj} &= \left\langle \delta_w^{(\imath)}\vec{e}_{wtli}^{\,qV},\vec{h}_{ctn'm'}^{\,p'q'}\right\rangle \\ &= \begin{cases}\left\langle \delta_w^{(\imath)}\vec{e}_{wtlm'}^{\,qV},\vec{h}_{ctn'm'}^{\,p'q'}\right\rangle & \text{if } i=m'\\ 0 & \text{otherwise}\end{cases} \quad (9)\end{aligned}$$

$$\begin{aligned}\left(T_H^{(\imath)V}\right)_{kj} &= \left\langle \vec{e}^{\,p'q'}_{ctn'm'}, \delta_w^{(\imath)} \vec{h}^{\,qV}_{wtli} \right\rangle \\ &= \begin{cases} \left\langle \vec{e}^{\,p'q'}_{ctn'm'}, \delta_w^{(\imath)} \vec{h}^{\,qV}_{wtlm'} \right\rangle & \text{if } i = m' \\ 0 & \text{otherwise} \end{cases} \end{aligned} \tag{10}$$

where $\imath = 1, 2$; q and $q' = e, h$ and $p' = s, c$. $\left(\vec{e}^{\,p'q'}_{ctn'm'},\ \vec{h}^{\,p'q'}_{ctn'm'}\right)$ are the transverse fields of the k-th eigenmode in cylindrical region *II*. $\left(\vec{e}^{\,qV}_{ctli},\ \vec{h}^{\,qV}_{ctli}\right)$ represent the transverse fields of the j-th eigenmode in waveguide $W_\imath$ as given in Appendix B.

The mutual inner products contain integrations of the following forms

$$I = \int_0^{\pi/4} \exp^{\pm\gamma_{mi} z} \begin{Bmatrix} \cos\left(\dfrac{m\pi}{2a}(x+a)\right) \\ \sin\left(\dfrac{m\pi}{2a}(x+a)\right) \end{Bmatrix} \begin{Bmatrix} \cos(n\phi) \\ \sin(n\phi) \end{Bmatrix} d\phi$$

$$= \int_0^{\pi/4} \exp^{\pm\gamma_{mi}(r_1\cos\phi - a)} \begin{Bmatrix} \cos\left(\dfrac{m\pi}{2a}(r_1 \sin\phi + a)\right) \\ \sin\left(\dfrac{m\pi}{2a}(r_1 \sin + a)\right) \end{Bmatrix} \begin{Bmatrix} \cos(n\phi) \\ \sin(n\phi) \end{Bmatrix} d\phi \tag{11}$$

The integrations have been computed numerically, efficiently and accurately. Once the inner products are calculated, then from (5) and (6), the following equation is obtained

$$\begin{bmatrix} \mathbf{C^{II}} \\ \mathbf{D^{II}} \end{bmatrix} = \begin{bmatrix} \left[M_C^{(1)}\right] & \left[M_C^{(2)}\right] \\ \left[M_D^{(1)}\right] & \left[M_D^{(2)}\right] \end{bmatrix} \begin{bmatrix} \mathbf{A} \\ \mathbf{B} \end{bmatrix} \tag{12}$$

where $\left[M_C^{(\imath)}\right]$ and $\left[M_D^{(\imath)}\right]$, of size $N_C^{II} \times N_W^{(\imath)}$, are:

$$\begin{aligned}\left[M_C^{(1)}\right] &= \left\{\left[\Lambda_{EJ}^{II}\right] - \left[\lambda_{EY}^{II}\right]\left[\lambda_{HY}^{II}\right]^{-1}\left[\lambda_{HJ}^{II}\right]\right\}^{-1} \\ &\quad \cdot \left\{\left[T_E^A\right] - \left[\lambda_{EY}^{II}\right]\left[\lambda_{HY}^{II}\right]^{-1}\left[T_H^A\right]\right\} \end{aligned} \tag{13}$$

$$\begin{aligned}\left[M_C^{(2)}\right] &= \left\{\left[\Lambda_{EJ}^{II}\right] - \left[\lambda_{EY}^{II}\right]\left[\lambda_{HY}^{II}\right]^{-1}\left[\lambda_{HJ}^{II}\right]\right\}^{-1} \\ &\quad \cdot \left\{\left[T_E^B\right] - \left[\lambda_{EY}^{II}\right]\left[\lambda_{HY}^{II}\right]^{-1}\left[T_H^B\right]\right\} \end{aligned} \tag{14}$$

$$\left[M_D^{(1)}\right] = \left\{\left[\Lambda_{EY}^{II}\right] - \left[\lambda_{EJ}^{II}\right]\left[\lambda_{HJ}^{II}\right]^{-1}\left[\lambda_{HY}^{II}\right]\right\}^{-1} \cdot \left\{\left[T_E^A\right] - \left[\lambda_{EJ}^{II}\right]\left[\lambda_{HJ}^{II}\right]^{-1}\left[T_H^A\right]\right\} \quad (15)$$

$$\left[M_D^{(2)}\right] = \left\{\left[\Lambda_{EY}^{II}\right] - \left[\lambda_{EJ}^{II}\right]\left[\lambda_{HJ}^{II}\right]^{-1}\left[\lambda_{HY}^{II}\right]\right\}^{-1} \cdot \left\{\left[T_E^B\right] - \left[\lambda_{EJ}^{II}\right]\left[\lambda_{HJ}^{II}\right]^{-1}\left[T_H^A\right]\right\} \quad (16)$$

with

$$\left[T_v^A\right] = \left(\left[T_v^{(1)B}\right] \; \left[T_v^{(2)F}\right]\right) \quad (17)$$

$$\left[T_v^B\right] = \left(\left[T_v^{(1)F}\right] \; \left[T_v^{(2)B}\right]\right) \quad (18)$$

and $v = E, H$.

From (12) and (1), the generalized scattering matrix $[S^P]$ of the cylindrical post in a rectangular waveguide can be obtained as

$$\begin{bmatrix} \mathbf{B^{(1)}} \\ \mathbf{B^{(2)}} \end{bmatrix} = \begin{bmatrix} \left[S_{11}^P\right] & \left[S_{12}^P\right] \\ \left[S_{21}^P\right] & \left[S_{22}^P\right] \end{bmatrix} \begin{bmatrix} \mathbf{A^{(1)}} \\ \mathbf{A^{(2)}} \end{bmatrix} = \left[S^P\right] \begin{bmatrix} \mathbf{A^{(1)}} \\ \mathbf{A^{(2)}} \end{bmatrix} \quad (19)$$

To have a solution for $\left[S^P\right]$, the following condition has to hold

$$N_C^{II} = N_W^{(1)} + N_W^{(2)} \quad (20)$$

This condition states that the number of modes used in region II has to be equal to the total number of modes used in waveguide regions W_1 and W_2. However, satisfying condition (20) is not enough for a non-singular solution of the scattering matrix. The eigenmodes of region II are orthogonal to the eigenmodes of the rectangular waveguide in the sense of the y-dependent eigenfunctions. The number of modes with certain y-variations in region I has to be equal to that of the modes with the same y-variations in waveguide regions. The second condition for mode selections is given by

$$N_{(n_y)}^{II} = N_{(n_y)}^{W_1} + N_{(n_y)}^{W_2} \quad (21)$$

A possible selection of modes which satisfy both conditions (20) and (21) is given in Table 2. The modes are arranged according to index.

Table 2. Type of wall, corresponding indices values and total number of modes for rectangular waveguide.

	PEW		PMW	
	TE	TM	TE	TM
l	$0, 2, 4, \cdots N_{xe}$	$2, 4, 6, \cdots N_{xe}$	$1, 3, 5, \cdots N_{xo}$	$1, 3, 5, \cdots N_{xo}$
i	$0, 1, 2, \cdots N_y$	$1, 2, 3, \cdots N_y$	$0, 1, 2, \cdots N_y$	$1, 2, 3, \cdots N_y$
N_W	$(\frac{1}{2}N_{xe}+1)N_y + N_y$	$\frac{1}{2}N_{xe}N_y$	$\frac{1}{2}(N_{xo}+1)(N_y+1)$	$\frac{1}{2}(N_{xo}+1)N_y$

In Table 2 N_{xe}, N_{xo} and N_y are the maximum even and odd indices in x-direction and y-direction for normal waveguide modes, respectively, N_W is the total number of modes in waveguide.

In Table 3, $f(\phi)$ is the ϕ variation dependence in the circular region which is chosen to satisfy the boundary condition on the walls at $\phi = 0$ and $\phi = 90°$, N_C is the total number of modes in cylindrical region.

Table 3. Type of wall (vertical-horizontal) and corresponding indices values for circular region.

	PEW-PEW		PMW-PMW		PMW-PEW	
	h	e	h	e	h	e
m	$1, 2, \cdots, N_y$	$0, 1, 2, \cdots, N_y$	$1, 2, 3, \cdots, N_y$	$0, 1, 2, \cdots, N_y$	$1, 2, 3, \cdots, N_y$	$0, 1, 2, \cdots, N_y$
n	$0, 2, \cdots, N_\phi$	$2, 4, \cdots, N_\phi$	$2, 4, \cdots, N_\phi$	$0, 2, 4, \cdots, N_\phi$	$1, 3, \cdots, N_\phi$	$1, 3, 5, \cdots, N_\phi$
N_ϕ	$2N_{xe}+2$	$2N_{xe}$	$2N_{xo}+2$	$2N_{xo}$	$N_{xe}+N_{xo}+2$	$N_{xe}+N_{xo}$
N_C	$(\frac{1}{2}N_\phi+2)N_y$	$\frac{1}{2}N_\phi(N_y+1)$	$(\frac{1}{2}N_\phi+1)N_y$	$(\frac{1}{2}N_\phi+1)(N_y+1)$	$\frac{1}{2}(N_\phi+3)N_y$	$\frac{1}{2}(N_\phi+1)(N_y+1)$
$f(\phi)$	cos	sin	sin	*cos*	cos	sin

3. N-PORTS GENERALIZED SCATTERING MATRIX

The generalized scattering matrices of the quarter of the structure, right angle bend, are combined together to get the generalized scattering matrix of the four port structure. The approach is valid only for any four port structure if symmetry planes are defined such that the structure is divided into identical quarters. Let us consider a four port structure that has two planes of symmetry perpendicular to each other as shown in Fig. 3a. Let the incident and reflected coefficient in each port be represented by A_i and B_i respectively where i is the port number as shown in Fig. 3a.

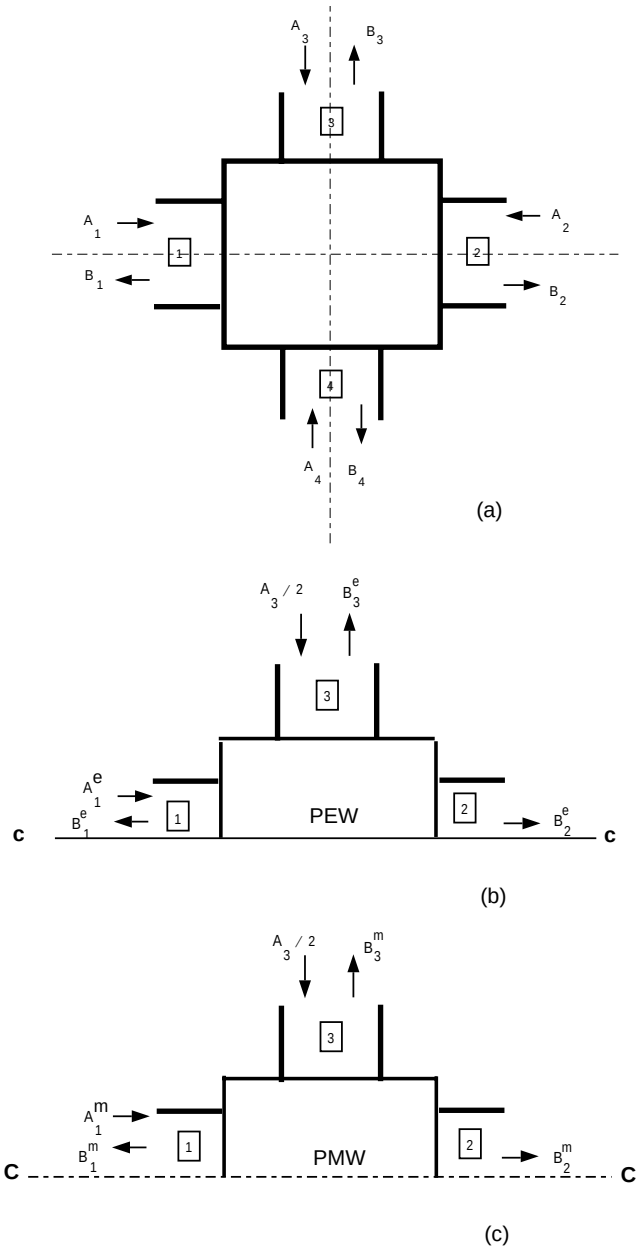

Figure 3. (a) Four ports structure with incident and reflected waves. (b) Short circuit along the symmetry line *c*-*c*. (c) Open circuit along the symmetry line *c*-*c*.

The reflection and incident coefficients are related by a generalized scattering matrix of a four port structure.

$$\begin{pmatrix} [B_1] \\ [B_2] \\ [B_3] \\ [B_4] \end{pmatrix} = \begin{pmatrix} [S_{11}] & [S_{12}] & [S_{13}] & [S_{14}] \\ [S_{21}] & [S_{22}] & [S_{23}] & [S_{24}] \\ [S_{31}] & [S_{32}] & [S_{33}] & [S_{34}] \\ [S_{41}] & [S_{42}] & [S_{43}] & [S_{44}] \end{pmatrix} \begin{pmatrix} [A_1] \\ [A_2] \\ [A_3] \\ [A_4] \end{pmatrix} \tag{22}$$

The generalized scattering matrix is obtained taking advantage of the existence of two perpendicular symmetry planes.

If two signals of amplitude $\frac{1}{2}A_3$ and *out* of phase are applied at arms 3 and 4, by symmetry a voltage minimum occurs at every point on the line of symmetry. This is the equivalent of a short circuit as shown in Fig. 3b. As the line of symmetry *c-c* passes through ports 1 and 2, then the modes in these ports will be those corresponding to the existence of an electric wall through these ports (Hence, the superscript 'e' in the notation of incident and reflection coefficients).

If two signals of amplitude $\frac{1}{2}A_3$ and *in* phase are applied at arms 3 and 4, by symmetry a voltage maximum occurs at every point on the line of symmetry. This is the equivalent of an open circuit as shown in Fig. 3c. The modes in ports 1 and 2 will be those corresponding to the existence of a magnetic wall passing through these ports (Hence, the superscript 'm' in the notation of incident and reflection coefficients).

In Fig. 3(b,c), the problem is reduced to that of a three ports network. Still the structure shown in Fig. 3b has another symmetry plane. If two signals of amplitude $\frac{1}{2}A_1$ and *out* of phase are applied at arms 1 and 2 of the structure shown in Fig. 3a, by symmetry a voltage minimum occurs at every point on the line of symmetry. This is the equivalent of a short circuit as shown in Fig. 4. Since the line of symmetry *d-d* passes through ports 3 and 4, then the modes in these ports will be those corresponding to the existence of an electric wall passing through these ports (The superscript 'e' is used in the notation of incident fields and the superscript 'ee' in the notation of reflected fields to refer to the presence of two symmetry plane of type PEW).

Also, if two signals of amplitude $\frac{1}{2}A_1$ and in phase are applied at arms 1 and 2 of the structure shown in Fig. 3a, by symmetry a voltage maximum occurs at every point on the line of symmetry. This is the equivalent of an open circuit as shown in Fig. 5

The same applies for the structure shown in Fig. 3c giving the cases shown in Figs. 6, 7. In all cases shown in Figs. 4–7, the problem is reduced to that of a two ports network.

From Fig. 3b, Fig. 4 and Fig. 5, it is clear that for ports 1 and 2, $B_i^e = B_i^{ee} + B_i^{me}$, also from Fig. 3c, Fig. 6 and Fig. 7 that

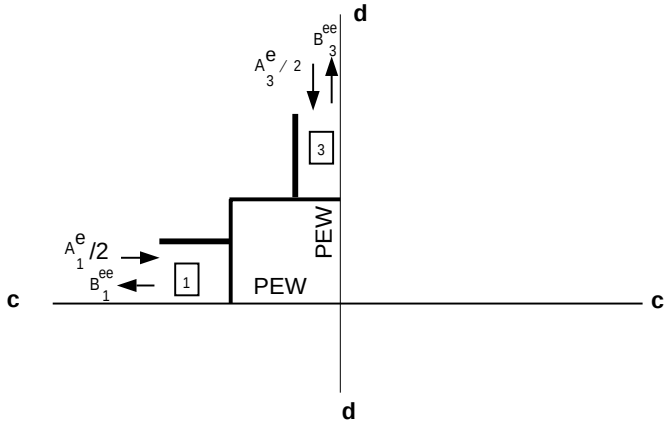

Figure 4. Short circuit along the symmetry line *c*-*c*, and symmetry line *d*-*d*.

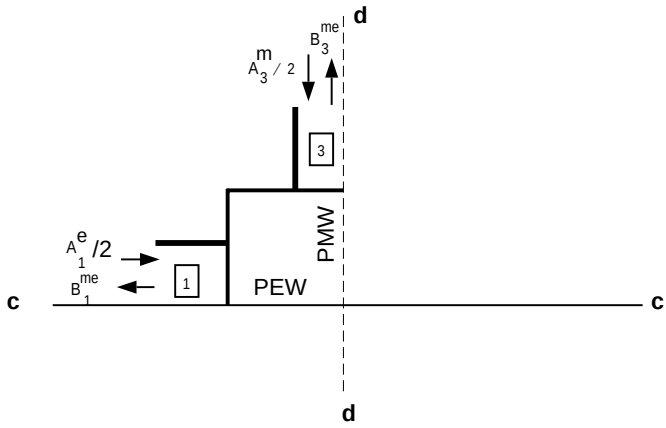

Figure 5. Short circuit along the symmetry line *c*-*c*, and open circuit along the symmetry line *d*-*d*.

$B_i^m = B_i^{em} + B_i^{mm}$

$$[B_i] = \begin{pmatrix} B_i^m \\ B_i^e \end{pmatrix} = \begin{pmatrix} B_i^{em} + B_i^{mm} \\ B_i^{ee} + B_i^{me} \end{pmatrix}; \quad i = 1, 2 \tag{23}$$

From Fig. 3(b,c), it is clear that for ports 3 and 4, $B_i = B_i^e + B_i^m$.

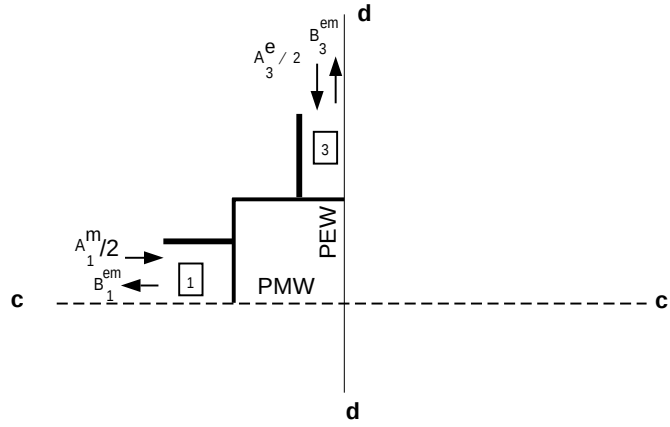

Figure 6. Open circuit along the symmetry line *c*-*c*, and short circuit along the symmetry line *d*-*d*.

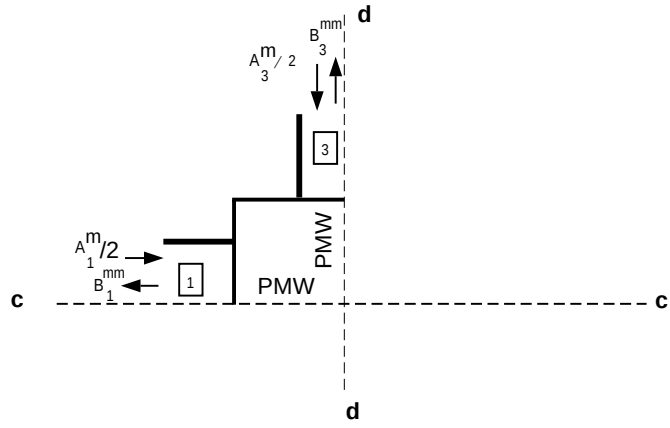

Figure 7. Open circuit along the symmetry line *c*-*c*, and symmetry line *d*-*d*.

From Figs. 6, 7; $B_i^m = \begin{pmatrix} B_i^{mm} \\ B_i^{em} \end{pmatrix}$. From Figs. 4, 5; $B_i^e = \begin{pmatrix} B_i^{me} \\ B_i^{ee} \end{pmatrix}$

$$[B_i] = \begin{pmatrix} B_i^{me} + B_i^{mm} \\ B_i^{ee} + B_i^{em} \end{pmatrix}; \quad i = 3, 4 \tag{24}$$

From Fig. 3(b,c);

$$[A_i] = \begin{pmatrix} A_i^m \\ A_i^e \end{pmatrix}; \quad i = 1, 2 \tag{25}$$

and from Figs. 4, 5

$$[A_i] = \begin{pmatrix} A_i^m \\ A_i^e \end{pmatrix}; \quad i = 3, 4 \tag{26}$$

where i is the port number, A_i^m is the vector coefficient of all modes TE and TM with odd indices in x-direction (Table 2) corresponding to PMW passing through the i-th port and the modes are arranged according to index. A_i^e is the vector coefficient of all modes TE and T M with even indices in x-direction (Table 2) corresponding to PEW passing through the i-th port and the modes are arranged according to index. Let us consider the case of PMW-PMW with incident and reflected waves as shown in Fig. 8. The reflection coefficient can be written in terms of the incident coefficient through the following relation:

$$\begin{aligned}
B_1^{mm} &= \frac{1}{2}\{S'_{11}(A_1^m + A_2^m) + S'_{12}(A_1^m + A_2^m) \\
&\quad + S'_{13}(A_3^m + A_4^m) + S'_{14}(A_3^m + A_4^m)\} \\
B_2^{mm} &= \frac{1}{2}\{S'_{21}(A_1^m + A_2^m) + S'_{22}(A_1^m + A_2^m) \\
&\quad + S'_{23}(A_3^m + A_4^m) + S'_{24}(A_3^m + A_4^m)\} \\
B_3^{mm} &= \frac{1}{2}\{S'_{31}(A_1^m + A_2^m) + S'_{32}(A_1^m + A_2^m) \\
&\quad + S'_{33}(A_3^m + A_4^m) + S'_{34}(A_3^m + A_4^m)\} \\
B_4^{mm} &= \frac{1}{2}\{S'_{41}(A_1^m + A_2^m) + S'_{42}(A_1^m + A_2^m) \\
&\quad + S'_{43}(A_3^m + A_4^m) + S'_{44}(A_3^m + A_4^m)\}
\end{aligned} \tag{27}$$

But, from Fig. 7, the reflected waves out of ports 1 and 3 are related to the incident waves in ports 1 and 3 through the formula:

$$\begin{pmatrix} B_1^{mm} \\ B_3^{mm} \end{pmatrix} = \frac{1}{2} \begin{pmatrix} S_{11}^{mm} & S_{12}^{mm} \\ S_{21}^{mm} & S_{22}^{mm} \end{pmatrix} \begin{pmatrix} A_1^m \\ A_3^m \end{pmatrix} \tag{28}$$

By assuming A_1^m and A_3^m to be the inputs to ports 2 and 4 respectively,

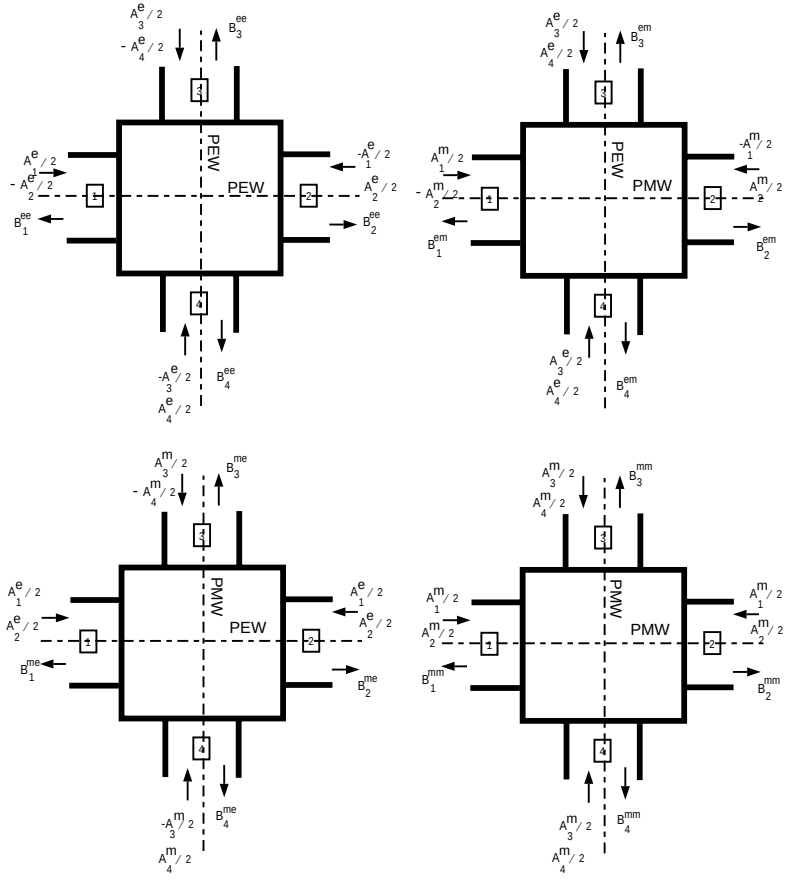

Figure 8. *H*-plane crossed waveguide junction, shown the different cases of quarter structures with the corresponding inputs and outputs.

then

$$\begin{pmatrix} B_2^{mm} \\ B_4^{mm} \end{pmatrix} = \frac{1}{2} \begin{pmatrix} S_{11}^{mm} & S_{12}^{mm} \\ S_{21}^{mm} & S_{22}^{mm} \end{pmatrix} \begin{pmatrix} A_1^m \\ A_3^m \end{pmatrix} \tag{29}$$

From (28), (29) in (27) then

$$\begin{pmatrix} B_1^{mm} \\ B_2^{mm} \\ B_3^{mm} \\ B_4^{mm} \end{pmatrix} = \frac{1}{2} \begin{pmatrix} S_{11}^{mm} & S_{12}^{mm} \\ S_{11}^{mm} & S_{12}^{mm} \\ S_{21}^{mm} & S_{22}^{mm} \\ S_{21}^{mm} & S_{22}^{mm} \end{pmatrix} \begin{pmatrix} A_1'^m \\ A_3'^m \end{pmatrix} \tag{30}$$

where $A_1'^m = A_1^m + A_2^m$, $A_3'^m = A_3^m + A_4^m$. Similar relations for the other combinations shown in Fig. 8 are obtained. By substitution from (30) and similar relations in (23, 24) the following relations are obtained:

$$[B_1] = \frac{1}{2}\begin{pmatrix} S_{11}^{em}+S_{11}^{mm} & 0 & S_{11}^{mm}-S_{11}^{em} & 0 & 0 & S_{12}^{mm} & S_{12}^{em} & S_{12}^{mm} & S_{12}^{em} \\ 0 & S_{11}^{me}+S_{11}^{ee} & 0 & S_{11}^{me}-S_{11}^{ee} & S_{12}^{me} & S_{12}^{ee} & -S_{12}^{me} & -S_{12}^{ee} \end{pmatrix}[A] \quad (31)$$

$$[B_2] = \frac{1}{2}\begin{pmatrix} S_{11}^{mm}-S_{11}^{em} & 0 & S_{11}^{mm}+S_{11}^{em} & 0 & 0 & S_{12}^{mm} & -S_{12}^{em} & S_{12}^{mm} & -S_{12}^{em} \\ 0 & S_{11}^{me}-S_{11}^{ee} & 0 & S_{11}^{me}+S_{11}^{ee} & S_{12}^{me} & -S_{12}^{ee} & -S_{12}^{me} & S_{12}^{ee} \end{pmatrix}[A] \quad (32)$$

$$[B_3] = \frac{1}{2}\begin{pmatrix} S_{21}^{mm} & S_{21}^{me} & S_{21}^{mm} & S_{21}^{me} & S_{22}^{me}+S_{22}^{mm} & 0 & S_{22}^{mm}-S_{22}^{me} & 0 \\ S_{21}^{em} & S_{21}^{ee} & -S_{21}^{em} & S_{21}^{ee} & 0 & S_{22}^{em}+S_{22}^{ee} & 0 & S_{22}^{em}-S_{22}^{ee} \end{pmatrix}[A] \quad (33)$$

$$[B_4] = \frac{1}{2}\begin{pmatrix} S_{21}^{mm} & -S_{21}^{me} & S_{21}^{mm} & -S_{21}^{me} & S_{22}^{me}-S_{22}^{mm} & 0 & S_{22}^{mm}+S_{22}^{me} & 0 \\ S_{21}^{em} & -S_{21}^{ee} & -S_{21}^{em} & S_{21}^{ee} & 0 & S_{22}^{em}-S_{22}^{ee} & 0 & S_{22}^{em}+S_{22}^{ee} \end{pmatrix}[A] \quad (34)$$

where

$$[A] = (A_1^m \; A_1^e \; A_2^m \; A_2^e \; A_3^m \; A_3^e \; A_4^m \; A_4^e)^T \quad (35)$$

T is the transpose of matrix. From (31) to (34) the generalized scattering matrix of the four ports in terms of those of right bends is given by

$$\frac{1}{2}\left(\begin{array}{cc|cc} S_{11}^{mm}+S_{11}^{em} & 0 & S_{11}^{mm}-S_{11}^{em} & 0 \\ 0 & S_{11}^{me}+S_{11}^{ee} & 0 & S_{11}^{me}-S_{11}^{ee} \\ \hline S_{11}^{mm}-S_{11}^{em} & 0 & S_{11}^{mm}+S_{11}^{em} & 0 \\ 0 & S_{11}^{me}-S_{11}^{ee} & 0 & S_{11}^{me}+S_{11}^{ee} \\ \hline S_{21}^{mm} & S_{21}^{me} & S_{21}^{mm} & S_{21}^{me} \\ S_{21}^{em} & S_{21}^{ee} & -S_{21}^{em} & -S_{21}^{ee} \\ \hline S_{21}^{mm} & S_{21}^{me} & S_{21}^{mm} & S_{21}^{me} \\ S_{21}^{em} & -S_{21}^{ee} & -S_{21}^{em} & S_{21}^{ee} \end{array}\right)$$

$$\left(\begin{array}{cc|cc} S_{12}^{mm} & S_{12}^{em} & S_{12}^{mm} & S_{12}^{em} \\ S_{12}^{me} & S_{12}^{ee} & -S_{12}^{me} & -S_{12}^{ee} \\ \hline S_{12}^{mm} & -S_{12}^{em} & S_{12}^{mm} & -S_{12}^{em} \\ S_{12}^{me} & -S_{12}^{ee} & -S_{12}^{me} & S_{12}^{ee} \\ \hline S_{22}^{mm}+S_{22}^{me} & 0 & S_{22}^{mm}-S_{22}^{me} & 0 \\ 0 & S_{22}^{em}+S_{22}^{ee} & 0 & S_{22}^{em}-S_{22}^{ee} \\ \hline S_{22}^{mm}-S_{22}^{me} & 0 & S_{22}^{me}+S_{22}^{mm} & 0 \\ 0 & S_{22}^{em}+S_{22}^{ee} & 0 & S_{22}^{em}+S_{22}^{ee} \end{array}\right) \tag{36}$$

Each element of the matrix is a generalized matrix, e.g., S_{ij}^{me} represents the scattering parameter of the right angle bend in case of a horizontal PEW, vertical PMW and so on for other elements.

The generalized scattering matrix of the 4-ports structure in (22) is used to obtain that of the H-plane T junction by short circuiting the fourth port. Also, the generalized scattering matrix of the 90° bend is obtained from that of the 4 ports by short circuiting ports 2 and 4. the resulting generalized scattering matrices are as follows respectively

$$\left[S^{(3)}\right] = \left(\begin{array}{cc} [S_{11}]-[S_{14}][\alpha_{44}][S_{41}] & [S_{12}]-[S_{14}][\alpha_{44}][S_{42}] \\ [S_{21}]-[S_{24}][\alpha_{44}][S_{41}] & [S_{22}]-[S_{24}][\alpha_{44}][S_{42}] \\ [S_{31}]-[S_{34}][\alpha_{44}][S_{41}] & [S_{32}]-[S_{34}][\alpha_{44}][S_{42}] \end{array} \right. \left. \begin{array}{c} [S_{13}]-[S_{14}][\alpha_{44}][S_{43}] \\ [S_{23}]-[S_{24}][\alpha_{44}][S_{43}] \\ [S_{33}]-[S_{34}][\alpha_{44}][S_{43}] \end{array}\right) \tag{37}$$

where $[\alpha_{44}] = ([U]+[S_{44}])^{-1}$

$$\left[S^{(2)}\right] = \begin{pmatrix} [S_{11}] & [S_{13}] \\ [S_{31}] & [S_{33}] \end{pmatrix} - \begin{pmatrix} [S_{12}] & [S_{14}] \\ [S_{32}] & [S_{34}] \end{pmatrix} \cdot \begin{pmatrix} [U]+[S_{22}] & [S_{24}] \\ [S_{42}] & [U]+[S_{44}] \end{pmatrix}^{-1} \begin{pmatrix} [S_{21}] & [S_{23}] \\ [S_{41}] & [S_{43}] \end{pmatrix} \tag{38}$$

$[U]$ is the identity matrix.

4. NUMERICAL SOLUTION VERIFICATION

A computer program has been developed to implement the modeling presented in the previous sections for computing the generalized

scattering matrix of a cylindrical post in a waveguide junction. As a verification of the modeling and the program, the results for a conducting post in crossed waveguides junction, T-junction and right-angle bend are presented in this section.

4.1. Crossed Waveguides Junction Results

To verify the correctness of the modeling and the program, the convergence is examined first. Fig. 9 gives the convergence of the dominant mode S-parameters of centered conducting post in crossed waveguide junctions varying the number of modes used, where N_x and N_y are the mode index numbers in x-direction and y-direction in the waveguide, respectively. The number of modes used in region **II** are determined in terms of N_x and N_y according to the conditions for mode selections presented before. While the maximum index for y-variation in region **I** is given by $N_y^{II} = N_y \cdot (b_2 - b_1)/b$ for better convergence [27, 28]. The figure shows that the numerical results are converged for small values of N_x and N_y.

The S-parameters for a small gap is shown in Fig. 10 and compared with a commercial package of finite element method and the results are in excellent agreement with it. The relation between the S-parameters and gap for a fixed frequency is shown in Fig. 11.

4.2. T-junction Results

The S-parameters for a gap equal to $0.024''$ is shown in Fig. 12. The relation between the S-parameters and gap for a fixed frequency is shown in Fig. 13.

4.3. Right-Bend Results

The S-parameters of Right-angle bend is shown for the case of a small gap in Fig. 14. The result were compared with FEM [12] and are in good agreement. The effect of the gap on the S-parameters for a fixed frequency is shown in Fig. 15.

4.4. Cylindrical Post in Rectangular Waveguide

For a cylindrical post in rectangular waveguide as shown in Fig. 1, the S-parameters were also obtained and compared to FEM as shown in Fig. 16. The results are in good agreement.

Also, if one side of the rectangular waveguide is shorted, the one port structure is obtained and the reflection coefficient is computed for

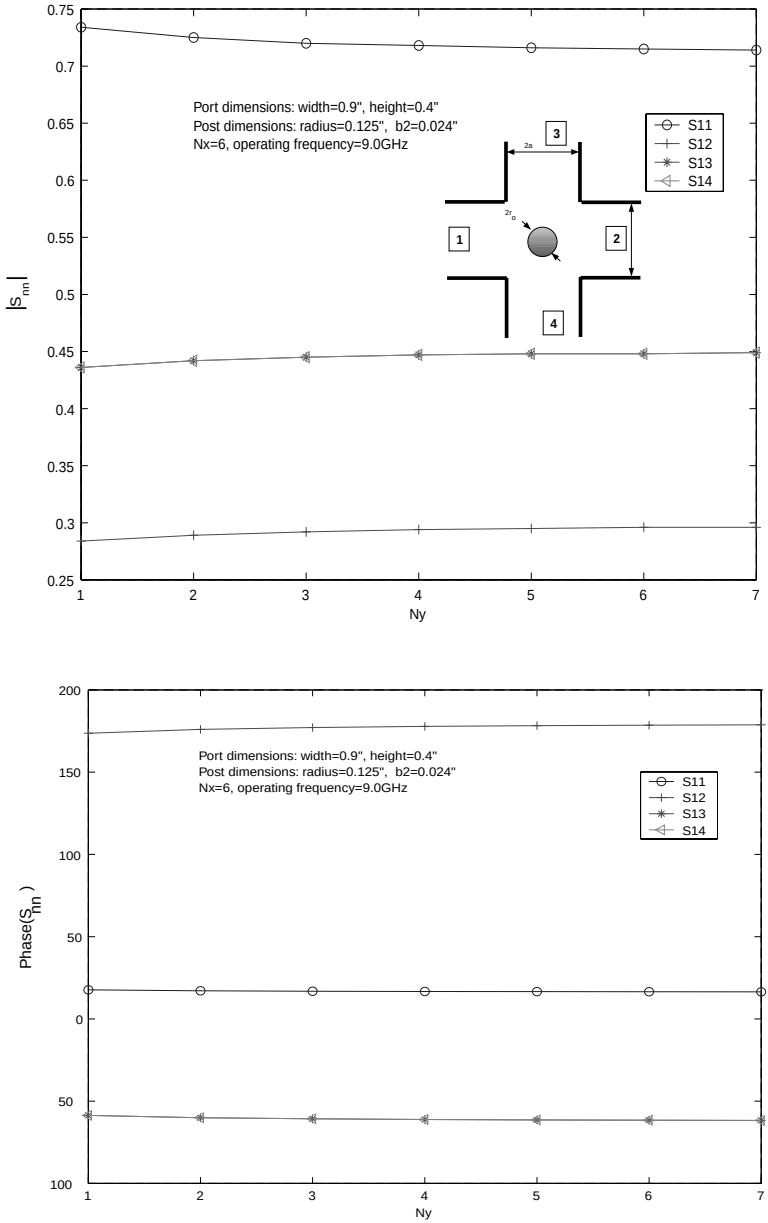

Figure 9. Convergence of the magnitude and the phase of the scattering parameters for a H-plane crossed waveguides junction operating in X-band with a gap $= 0.024''$, $b_1 = 0$.

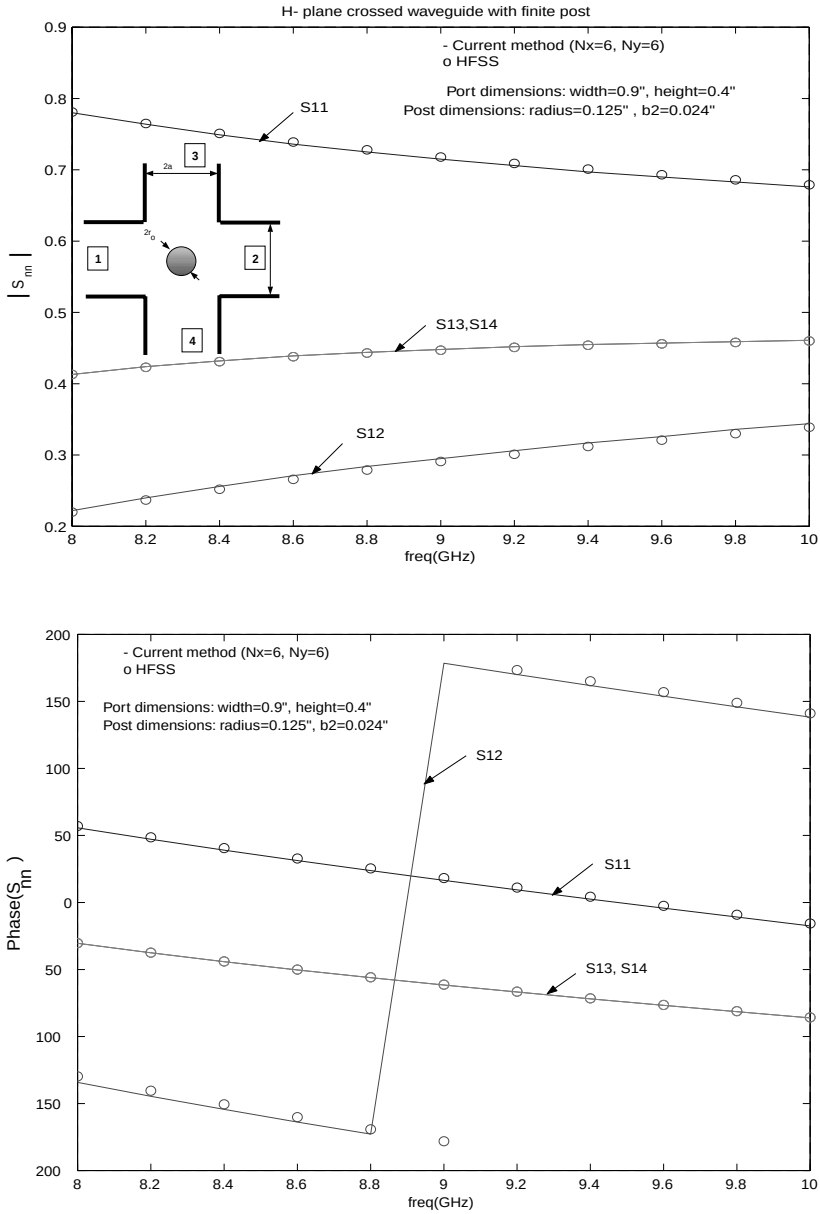

Figure 10. Magnitude and phase of the scattering parameters, as a function of frequency, for a H-plane crossed waveguides junction operating in X-band with a gap $= 0.024''$, $b_1 = 0$.

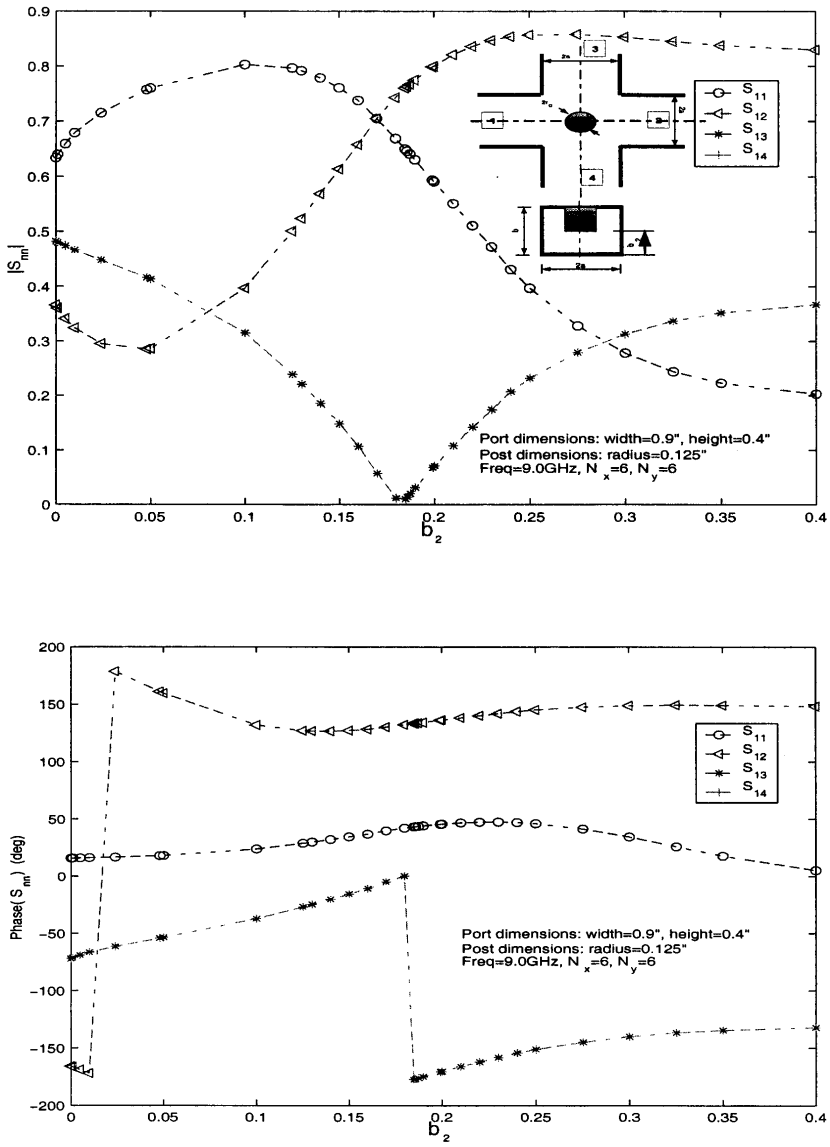

Figure 11. Magnitude and phase of the scattering parameters, as a function of the post gap, for a H-plane crossed waveguides junction operating in X-band.

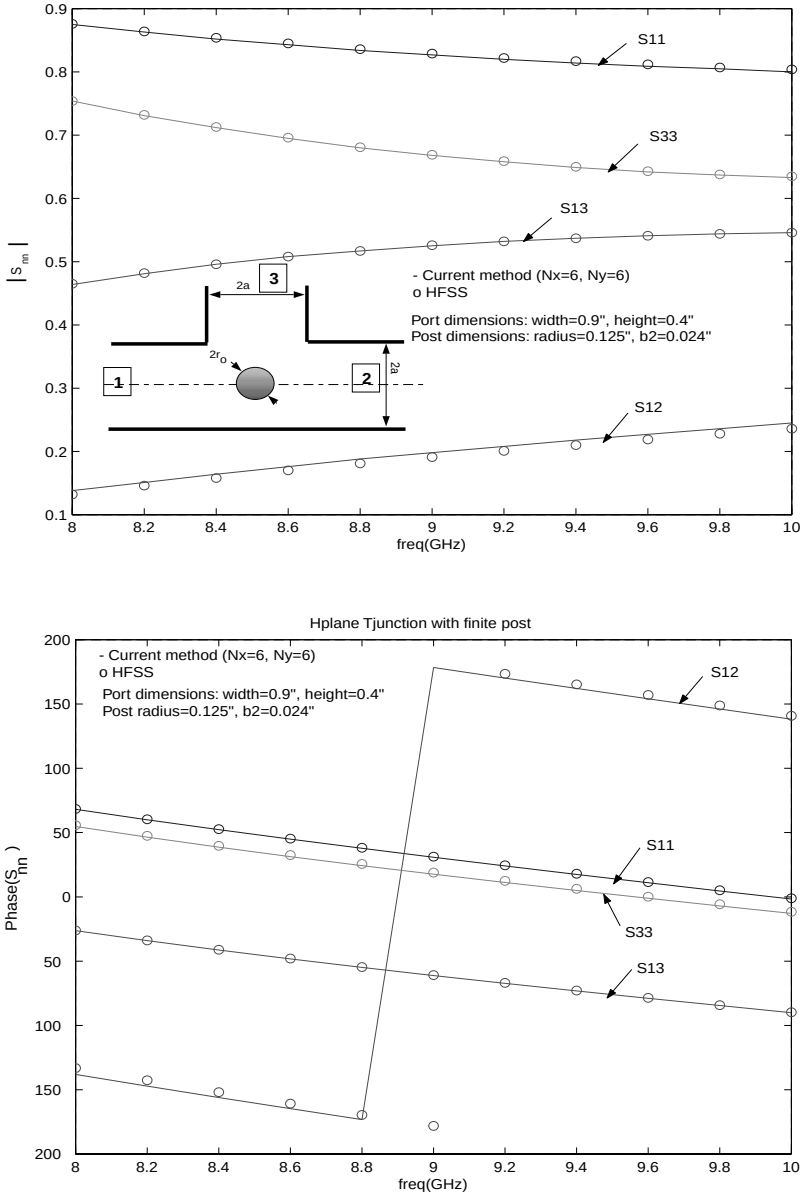

Figure 12. Magnitude and phase of the scattering parameters, as a function of frequency, for a H-plane T-junction operating in X-band with a gap $= 0.024''$.

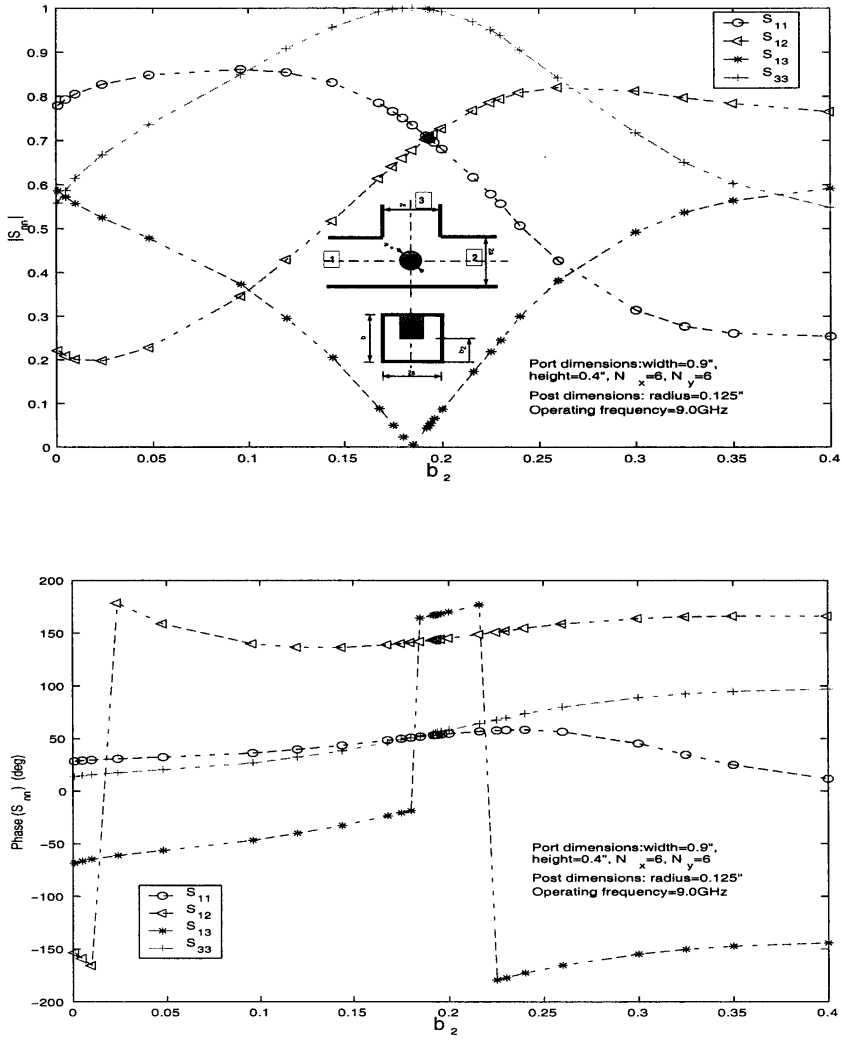

Figure 13. Magnitude and phase of the scattering parameters, as a function of the post gap, for a H-plane T-junction operating in X-band.

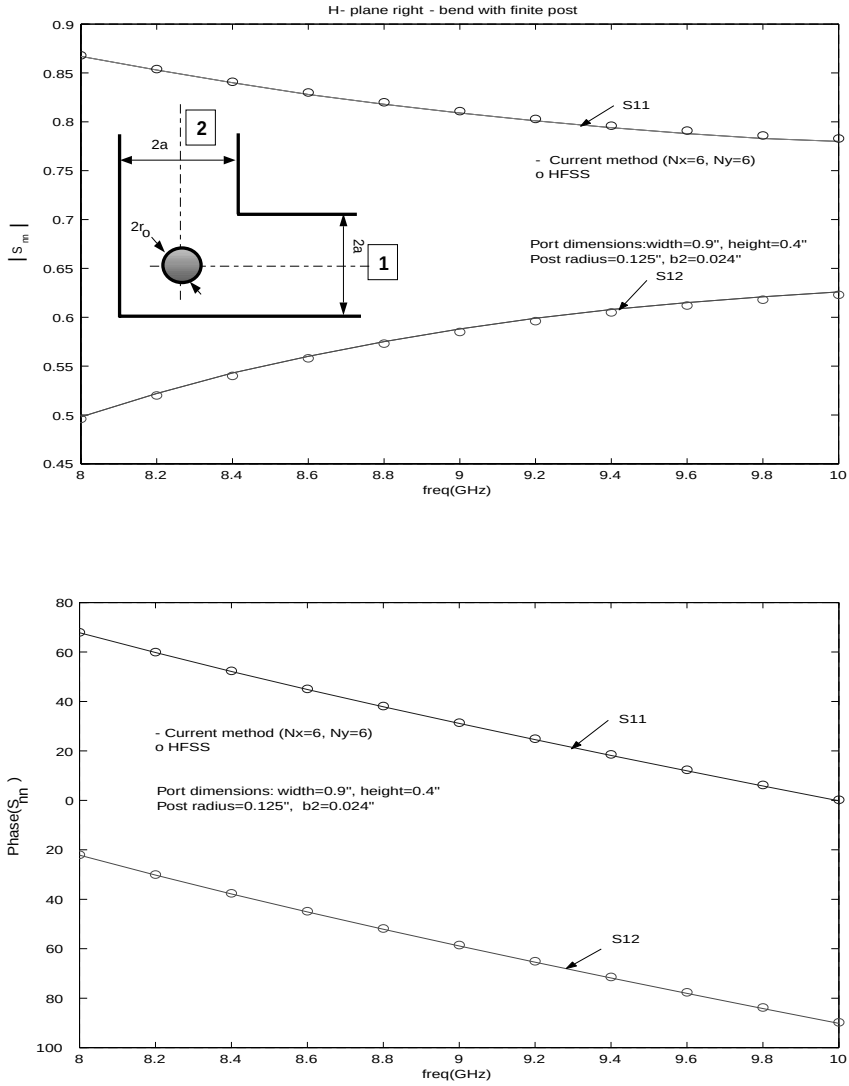

Figure 14. Magnitude and phase of the scattering parameters, as a function of frequency, for a H-plane right-bend operating in X-band with a gap $= 0.024''$.

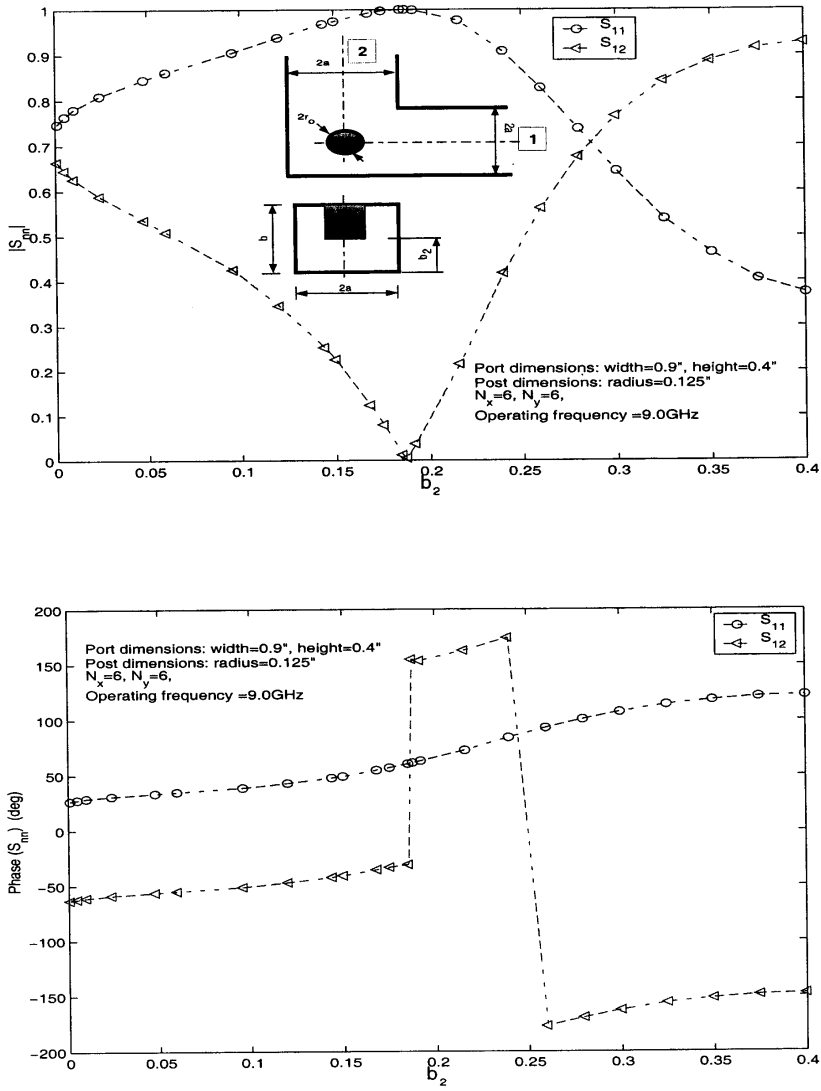

Figure 15. Magnitude and phase of the scattering parameters, as a function of the post gap, for a H-plane right-bend operating in X-band.

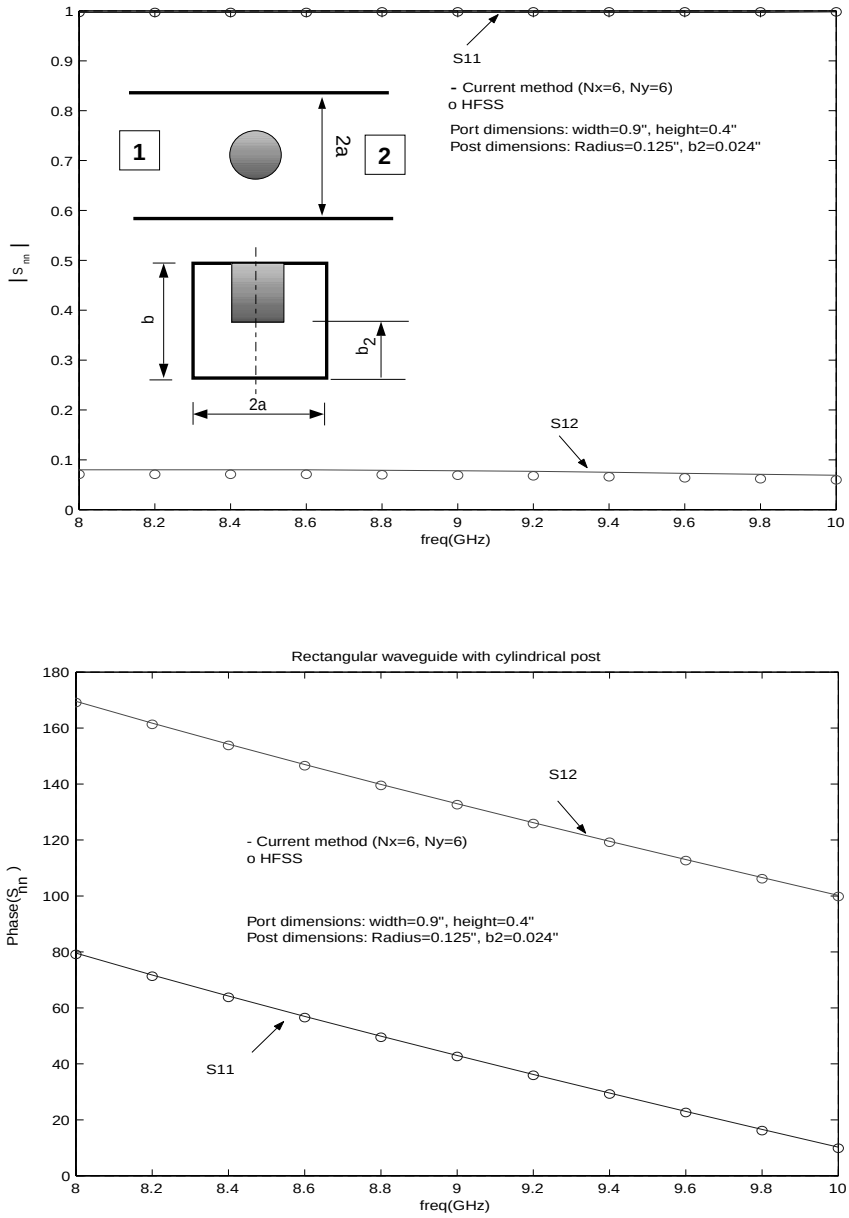

Figure 16. The scattering parameters of a cylindrical post in a rectangular post in a rectangular waveguide operating in X-band.

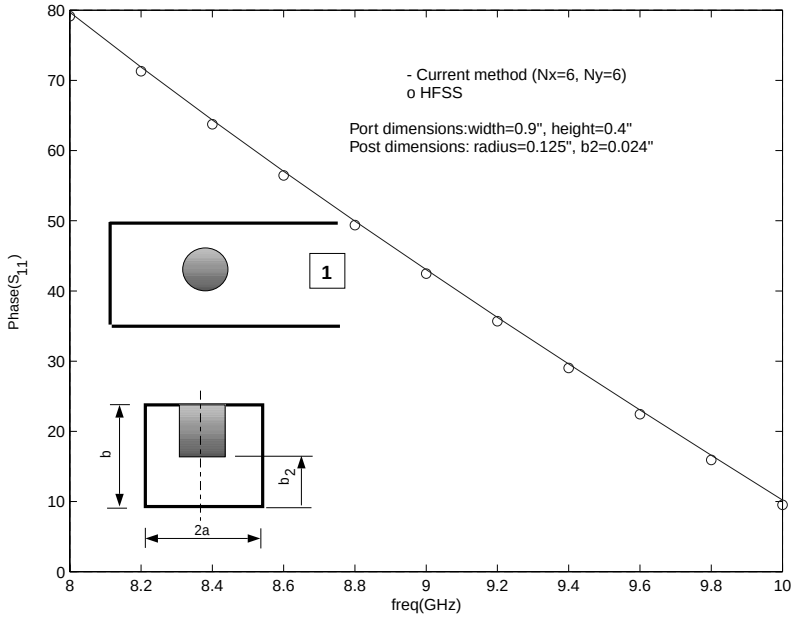

Figure 17. The scattering parameters of a cylindrical post in a rectangular waveguide one side shorted, operating in X-band.

this case as shown in Fig. 17. The results are in good agreement with the FEM.

5. CONCLUSION

A rigorous method for computing the generalized scattering matrix of conducting posts in rectangular waveguide junctions is presented. From all the results obtained it can be concluded that the method is correct and accurate as verified by the simulation results. The method is so useful as many structures (Fig. 1) can be obtained from just one structure by short circuiting different ports which verifies the correctness of the higher order modes of the obtained generalized scattering matrix. The method is also efficient as the computation time of this method is about two order of magnitudes faster than FEM [12]. This can be considered as an efficient tool for filter design and other applications such as coupling computation between combline cavities.

APPENDIX A. FIELD EXPRESSIONS IN RADIAL WAVEGUIDE REGION

$$\vec{E}_{ct}^{\,q} = \sum_n \sum_m \left\{ C_{nm}^{qe} \frac{J_n(\xi_m^{qe}\rho)}{J_n(\xi_m^{qe} r_0)} + D_{nm}^{qe} \frac{Y_n(\xi_m^{qe}\rho)}{Y_n(\xi_m^{qe} r_0)} \right\} \vec{e}_{ctnm}^{\,qe}(\rho,\phi,y) + \sum_n \sum_m \left\{ C_{nm}^{qh} \frac{J_n'(\xi_m^{qh}\rho)}{J_n'(\xi_m^{qh} r_0)} + D_{nm}^{qh} \frac{Y_n'(\xi_m^{qh}\rho)}{Y_n'(\xi_m^{qh} r_0)} \right\} \vec{e}_{ctnm}^{\,qh}(\rho,\phi,y) \quad \text{(A1)}$$

$$\vec{H}_{ct}^{\,q} = \sum_n \sum_m \left\{ C_{nm}^{qe} |\xi_m^{qe}| \frac{J_n'(\xi_m^{qe}\rho)}{J_n(\xi_m^{qe} r_0)} + D_{nm}^{qe} |\xi_m^{qe}| \frac{Y_n'(\xi_m^{qe}\rho)}{Y_n(\xi_m^{qe} r_0)} \right\} \vec{h}_{ctnm}^{\,qe}(\rho,\phi,y) + \sum_n \sum_m \left\{ C_{nm}^{qh} \frac{J_n(\xi_m^{qh}\rho)}{|\xi_m^{qh}| J_n'(\xi_m^{qh} r_0)} + D_{nm}^{qh} \frac{Y_n(\xi_m^{qh}\rho)}{|\xi_m^{qh}| Y_n(\xi_m^{qh} r_0)} \right\} \vec{h}_{ctnm}^{\,qh}(\rho,\phi,y) \quad \text{(A2)}$$

$$\xi_m^{qv2} = k^2 - k_m^{qv2} = k_0^2 \epsilon_r - k_m^{qv2} \quad \text{(A3)}$$

The coefficients D_{nm}^{qe} and D_{nm}^{qh} are zero for region I (because of the $\rho = 0$ point in region I, the second kind of Bessel functions should be excluded). J_n and Y_n are either the first kind and the second kind Bessel functions or the first kind and the second kind modified Bessel junctions depending on the sign of ξ_m^{qv2} $(v = e, h)$; J_n' and Y_n' are the derivatives of J_n and Y_n respectively; $q = I$ or II. $\vec{e}_{ctnm}^{\,qv}$ and $\vec{h}_{ctnm}^{\,qv}$ represent the transverse electric and magnetic field of TE_y mode $(v = h)$ or TM_y mode $(v = e)$ of parallel planes bounded in y direction in the cylindrical coordinate system (ρ, ϕ, y).

For TE_y mode

$$\vec{e}_{ctnm}^{\,qh}(\rho,\phi,y) = \hat{\phi} \frac{1}{\sqrt{\lambda_{nm}^{qh}}} \frac{1}{{\xi_m^{qh}}^2} \Phi_n^{ph}(\phi) h_{ym}^{qh}\left(k_m^{qh}, y\right) \quad \text{(A4)}$$

$$j\omega\mu \vec{h}_{ctnm}^{\,qh}(\rho,\phi,y) = \hat{y} \frac{1}{\sqrt{\lambda_{nm}^{qh}}} \Phi_n^{ph}(\phi) h_{ym}^{qh}\left(k_m^{qh}, y\right) + \hat{\phi} \frac{1}{\sqrt{\lambda_{nm}^{qh}}} \frac{1}{{\xi_m^{qh}}^2} \frac{\partial^2}{\rho \partial\phi \partial y} \cdot \left\{ \Phi_n^{ph}(\phi) h_{ym}^{qh}\left(k_m^{qh}, y\right) \right\} \quad \text{(A5)}$$

where $\hat{y}$ and $\hat{\phi}$ are the unit vectors in y and ϕ directions respectively.

where

$$\Phi_n^{ph} = \begin{cases} \cos(n\phi) & n = 0, 1, 2, \cdots \quad \text{if } p = c \\ -\sin(n\phi) & n = 1, 2, \cdots \quad \text{if } p = s \end{cases} \quad \text{(A6)}$$

$$h_{ym}^{qh}\left(k_m^{qh},y\right) = \begin{cases} \sin\left(k_m^{Ih}(y-b_1)\right) & k_m^{Ih}=\dfrac{m\pi}{b_2-b_1} \quad \text{region } I \\ \sin\left(k_m^{IIh}y\right) & k_m^{IIh}=\dfrac{m\pi}{b} \quad \text{region } II \end{cases} \tag{A7}$$

For TM_y mode

$$\vec{e}_{ctnm}^{qe}(\rho,\phi,y) = \hat{y}\frac{1}{\sqrt{\lambda_{nm}^{qe}}}\Phi_n^{pe}(\phi)e_{ym}^{qe}\left(k_m^{qe},y\right)+\hat{\phi}\frac{1}{\sqrt{\lambda_{nm}^{qe}}}\frac{1}{\xi_m^{qe2}}\frac{\partial^2}{\rho\partial\phi\partial y} \cdot\left\{\Phi_n^{pe}(\phi)e_{ym}^{qe}\left(k_m^{qe},y\right)\right\} \tag{A8}$$

$$j\omega\mu\vec{h}_{ctnm}^{qe}(\rho,\phi,y) = \hat{\phi}\frac{1}{\sqrt{\lambda_{nm}^{qe}}}\frac{1}{\xi_m^{qe2}}\Phi_n^{pe}(\phi)e_{ym}^{qe}\left(k_m^{qe},y\right) \tag{A9}$$

where

$$\Phi_n^{pe} = \begin{cases} \sin(n\phi) & n=1,2,\cdots \quad \text{if } p=s \\ \cos(n\phi) & n=0,1,2,\cdots \quad \text{if } p=c \end{cases} \tag{A10}$$

$$e_{ym}^{qe}\left(k_m^{qe},y\right) = \begin{cases} \cos\left(k_m^{Ie}(y-b_1)\right) & k_m^{Ie}=\dfrac{m\pi}{b_2-b_1} \quad \text{region } I \\ \sin\left(k_m^{IIe}y\right) & k_m^{IIe}=\dfrac{m\pi}{b} \quad \text{region } II \end{cases} \tag{A11}$$

and λ_{nm}^{v} are normalizations defined by

$$\lambda_{nm}^{v}=\int_0^{\pi/2}\int_{y1}^{y2}\left\{\vec{e}_{ctnm}^{qv}\times\vec{h}_{ctnm}^{qv}\right\}\cdot\hat{\rho}d\phi dy \tag{A12}$$

where $y_1=0,\ y_2=b$ in region I and $y_1=b_1,\ y_2=b_2$ in region II. The integration with respect to ϕ will be divided into two integrations one as $(0<\phi<\pi/4)$ and the other one as $(\pi/4<\phi<\pi/2)$

APPENDIX B. FIELD EXPRESSIONS IN RECTANGULAR WAVEGUIDE REGION

$$\begin{Bmatrix}\vec{E}_{wt}^{(1)}(x_1,y,z_1)\\ \vec{E}_{wt}^{(2)}(x_2,y,z_2)\end{Bmatrix} = \sum_{v=e,h}\sum_{l}\sum_{i}\left[\begin{Bmatrix}B_{li}^{(1)v}\\ A_{li}^{(2)v}\end{Bmatrix}\vec{e}_{wtli}^{\,vF}+\begin{Bmatrix}A_{li}^{(1)v}\\ B_{li}^{(2)v}\end{Bmatrix}\vec{e}_{wtli}^{\,vB}\right] \tag{B1}$$

$$\begin{Bmatrix}\vec{H}_{wt}^{(1)}(x_1,y,z_1)\\ \vec{H}_{wt}^{(2)}(x_2,y,z_2)\end{Bmatrix} = \sum_{v=e,h}\sum_{l}\sum_{i}\left[\begin{Bmatrix}B_{li}^{(1)v}\\ A_{li}^{(2)v}\end{Bmatrix}\vec{h}_{wtli}^{\,vF}+\begin{Bmatrix}A_{li}^{(1)v}\\ B_{li}^{(2)v}\end{Bmatrix}\vec{h}_{wtli}^{\,vB}\right] \tag{B2}$$

where $v = e$ and h represent TM and TE modes in the waveguide, respectively. The transverse fields of an eigenmode are given by:

$$\begin{aligned} & \left\{ \begin{array}{l} \vec{e}^{vFR}_{wtli}(x_R, y, z_R) \\ \vec{e}^{vBR}_{wtli}(x_R, y, z_R) \end{array} \right\} \\ = & \left[\hat{y} e^{vR}_{wyli}(x_R, y) + \hat{\phi} \left\{ \begin{array}{l} e^{vFR}_{w\phi li}(x_R, y) \\ e^{vBR}_{w\phi li}(x_R, y) \end{array} \right\} \right] \exp^{\mp \gamma_{li} z} \qquad \text{(B3)} \\ & j\omega\mu \left\{ \begin{array}{l} \vec{h}^{vFR}_{wtli}(x_R, y, z_R) \\ \vec{h}^{vBR}_{wtli}(x_R, y, z_R) \end{array} \right\} \\ = & \left[\pm \hat{y} h^{vR}_{wyli}(x_R, y) + \hat{\phi} \left\{ \begin{array}{l} h^{vFR}_{w\phi li}(x_R, y) \\ h^{vBR}_{w\phi li}(x_R, y) \end{array} \right\} \right] \exp^{\mp \gamma_{li} z} \qquad \text{(B4)} \end{aligned}$$

where

$$\left\{ \begin{array}{l} e^{vFR}_{w\phi li}(x_R, y) \\ e^{vBR}_{w\phi li}(x_R, y) \end{array} \right\} = e^{vR}_{wxli}(x_R, y) \cos\phi \mp e^{vR}_{wzli}(x_R, y) \sin\phi \qquad \text{(B5)}$$

$$\left\{ \begin{array}{l} h^{vFR}_{w\phi li}(x_R, y) \\ h^{vBR}_{w\phi li}(x_R, y) \end{array} \right\} = h^{vR}_{wxli}(x_R, y) \cos\phi \mp h^{vR}_{wzli}(x_R, y) \sin\phi \qquad \text{(B6)}$$

where

$$e^{vR}_{wzli}(x_R, y) = \left\{ \begin{array}{ll} \sin(k_{xl}(x_R + a)) \sin(k_{yi} y) & v = e \\ 0 & v = h \end{array} \right. \qquad \text{(B7)}$$

$$h^{vR}_{wzli}(x_R, y) = \left\{ \begin{array}{ll} 0 & v = e \\ \cos(k_{xl}(x_R + a)) \cos(k_{yi} y) & v = h \end{array} \right. \qquad \text{(B8)}$$

$$\gamma^2_{li} = k^2_{xl} + k^2_{yi} - k^2_0 \epsilon_r; \quad k_{xl} = \frac{l\pi}{2a}; \quad k_{yi} = \frac{i\pi}{b} \qquad \text{(B9)}$$

where $R = W_1,\ W_2$: the waveguide regions, (x_1, z_1) and (x_2, z_2) are the coordinates of the local cartesian systems related to the global cylindrical coordinate system, as shown in Fig. 2, by the following relations:

$$x_1 = r_1 \sin\phi,\ x_2 = r_1 \cos\phi,\ z_1 = r_1 \cos\phi - a,\ z_2 = a - r_1 \sin\phi \qquad \text{(B10)}$$

The indices l and i are given in Table 2. The other components of the fields can be found from the z-components. It should be

noted that the eigenmodes in the rectangular waveguides and the ones in the cylindrical interaction region have the same y-dependent eigenfunctions. Therefore, the eigenmodes in the two different regions are orthogonal in the sense of the y-dependent eigenfunctions.

REFERENCES

1. Liang, X.-P., K. A. Zaki, and A. E. Atia, "A rigorous three plane mode-matching technique for characterizing waveguide T-junctions and its application in multiplexer design," *IEEE Trans. Microwave Theory and Techniques,* Vol. 39, No. 12, 2138–2147, Dec. 1991.
2. Liang, X.-P., "Modeling of dual mode dielectric resonator filters and multiplexers," Ph.D. Dissertation, University of Maryland at College Park, 1993.
3. Pace, J. and R. Mittra, "Generalized scattering matrix analysis of waveguide discontinuity problems," in *Quasi-Optics XIV., Polytechnic Institute of Brooklyn Press,* 172–194, New York, 1964.
4. Simpson, G. R., "A generalized n-port cascade connection," *IEEE MTT-S Int. Microwave Symp. Digest,* 507–509, 1981.
5. Shih, Y.-C., T. Itoh, and L. Q. Bui, "Computer-aided design of millimeter-wave E-plane filters," *IEEE Trans. Microwave Theory Tech.,* Vol. MTT-31, 1135–1142, Feb. 1983.
6. Omar, A. S. and K. Schünemann, "Transmission matrix representation of finline discontinuities," *IEEE Trans. Microwave Theory Tech.,* Vol. MTT-33, 765–770, Sept. 1985.
7. Gesche, R. and N. Löchel, "Scattering by a lossy dielectric cylinder in a rectangular waveguide," *IEEE Trans. Microwave Theory Tech.,* Vol. MTT-36, 137–144, Jan. 1988.
8. Gesche, R. and N. Löchel, "Two cylindrical obstacles in a rectangular waveguide resonances and filter applications," *IEEE Trans. Microwave Theory Tech.,* Vol. MTT-37, 962–968, June 1989.
9. Liang, X.-P. and K. A. Zaki, "Modeling of cylindrical dielectric resonators in rectangular waveguide and cavities," *IEEE Trans. Microwave Theory Tech.,* Vol. MTT-41, 2174–2181, Dec. 1993.
10. Yao, H.-W., K. A. Zaki, A. E. Atia, and R. Hershtig, "Full wave modeling of conducting posts in rectangular waveguides and its applications to slot coupled combline filters," *IEEE Trans. Microwave Theory Tech.,* Vol. MTT-43, No. 12, Dec. 1995.
11. Yao, H.-W., "EM simulation of resonant and transmission

structures applications to filters and multiplexers," Ph.D. Dissertation, University of Maryland at College Park, 1995.

12. Agilent EEs of EDA, *Agilent High Frequency Structure Simulator 5.5,* December 1999.
13. Schwinger, J. and D. S. Saxon, *Discontinuities in Waveguides: Notes on Lectures by Julian Schwinger,* Gordon and Breach Science Publishers, New York, 1968.
14. Marcuvitz, N., *Waveguide Handbook,* M.I.T. Rad. Lab. Series, Vol. 10, 257–262, McGraw-Hill, New York, 1957.
15. Bradshaw, J. A., "Scattering from a round metal post and gap," *IEEE Trans. Microwave Theory Tech.,* Vol. MTT-21, 313–322, May 1973.
16. Okamoto, N., I. Nishioka, and Y. Nakanishi, "Scattering by a ferrimagnetic circular cylinder in a rectangular waveguide," *IEEE Trans. Microwave Theory Tech.,* Vol. MTT-19, 521–527, June 1971.
17. Cicconi, G. and C. Rosatelli, "Solutions of the vector wave equation for inhomogeneous dielectric cylinders-scattering in waveguide," *IEEE Trans. Microwave Theory Tech.,* Vol. MTT-25, 885–892, Nov. 1977.
18. Leviatan, Y., P. G. Li, A. T. Adams, and J. Perini, "Single-post inductive obstacle in rectangular waveguide," *IEEE Trans. Microwave Theory Tech.,* Vol. MTT-31, 806–812, Oct. 1983.
19. Li, P. G., A. T. Adams, Y. Leviatan, and J. Perini, "Multiple-post inductive obstacles in rectangular waveguide," *IEEE Trans. Microwave Theory Tech.,* Vol. MTT-32, 365–373, April 1984.
20. Leviatan, Y. and G. S. Sheaffer, "Analysis of inductive dielectric posts in rectangular waveguide," *IEEE Trans. Microwave Theory Tech.,* Vol. MTT-35, 48–59, Jan. 1987.
21. Khilla, A.-M. and I. Wolff, "Field theory treatment of H-plane waveguide junction with triangular ferrite post," *IEEE Trans. Microwave Theory Tech.,* Vol. MTT-26, 279–287, Apr. 1978.
22. Tasi, Y.-Y. and A. S. Omar, "Field theoretical treatment of H-plane waveguide junctions with anisotropic medium," *IEEE Trans. Microwave Theory Tech.,* Vol. MTT-40, 2164–2171, Dec. 1992.
23. Harrington, R. F., *Time-Harmonic Electromagnetic Fields,* McGraw-Hill, New York, 1961.
24. Kobayashi, Y. and M. Minegishi, "Precise design of a bandpass filter using high-Q dielectric ring resonators," *IEEE Trans. Microwave Theory Tech.,* Vol. MTT-35, 1156–1160, Dec. 1987.

25. Chen, S.-W. and K. A. Zaki, "Dielectric ring resonators loaded in waveguide and on substrate," *IEEE Trans. Microwave Theory Tech.,* Vol. MTT-39, 2069–2076, Dec. 1991.
26. Rizzi, P. A., *Microwave Engineering Passive Circuits,* Prentice Hall, Englewood Cliffs, NJ, 1988.
27. Mittra, R. and S. W. Lee, *Analytic Techniques in the Theory of Guided Waves,* Macmillan, New York, 1971.
28. Mansour, R. R. and R. H. MacPhie, "An improved transmission matrix formulation of cascaded discontinuities and its application to *E*-plane circuits," *IEEE Trans. Microwave Theory Tech.,* Vol. MTT-34, 1490–1498, Dec. 1986.